

Propagation characteristics and guiding of a high-power microwave in plasma waveguide

H. Ito,* C. Rajyaguru, N. Yugami, and Y. Nishida

Energy and Environmental Science, Graduate School of Engineering, Utsunomiya University, 7-1-2 Yoto, Utsunomiya, Tochigi 321-8585, Japan

T. Hosoya

Tochigi Nikon Corporation, 770 Mitori, Otawara, Tochigi 324-8625, Japan

(Received 15 February 2004; published 4 June 2004)

The propagation characteristics of a high-power microwave [electromagnetic (em) wave] in a plasma waveguide are reported. The plasma waveguide is formed by expanding plasmas via the ponderomotive force of the high-power microwave and the microwave pulse remains trapped within the plasma waveguide and is guided in it. With the increase of the incident microwave power, the width of the plasma waveguide increases and the half width of the radial electric field distribution decreases. This shows that the em wave modifies the refractive index of the plasma waveguide area. For a plasma waveguide with narrower width, the microwave propagates along the plasma waveguide at the fundamental TE mode, while as the waveguide width increases the higher mode component starts appearing. Analytical treatment to the propagation of the electromagnetic wave in a dielectric waveguide having a step-index profile and the numerical calculations for the radial distribution of the electric field show fairly good agreement with the results observed in the present experiments.

DOI: 10.1103/PhysRevE.69.066406

PACS number(s): 52.40.Db, 52.35.Mw, 52.40.Fd

I. INTRODUCTION

Advances in laser technology have led us to investigate the laser-matter interaction phenomena in a number of potential applications in fast ignition [1], compact x-ray lasers [2,3], high harmonic generation [4], and laser-plasma based particle accelerators [5,6]. The success of these applications depends critically on long interaction distances more than the Rayleigh length of high intensity laser pulses. For example, laser-plasma accelerators have been conceived to be the next generation particle accelerators with ultrahigh gradients. Proof-of-principle experiments have been performed and demonstrated ultrahigh field generation and electron accelerations by electron plasma waves at various universities and laboratories around the world [7–9].

Several methods of the laser guiding in a plasma channel have been proposed and demonstrated in order to extend the propagation distance of the laser beam beyond its diffraction limit. Plasma channels have been created by a variety of methods: (i) passing a long laser pulse through an axicon lens to create a line focus in a gas, which ionizes and heats the gas, creating a radially expanding hydrodynamic shock [10,11], (ii) using relativistic and/or ponderomotive self-channeling of an intense laser pulse in a plasma [12,13], and (iii) using a slow capillary discharge to control the plasma profile [14–18]. We have also performed the experiments of guiding an electromagnetic wave in a preformed plasma channel with the use of a high-power microwave instead of an intense laser pulse and demonstrated the guiding of the electromagnetic wave [19]. Essential idea involved in all the proposed concepts is to modify the refractive index of the plasma such that to have higher refractive index on axis and

lower off-axis area, which can be achieved with a plasma density profile that has a local minimum on axis. In all of above-mentioned schemes, the guiding conditions fix the electron plasma density and its spatial distribution. However, many applications require various plasma parameters for laser guidings. Thus, in order to control the propagation characteristic of laser pulses in the plasma channel with required characteristics, an investigation of relationships between plasma channel parameters and the propagation characteristic of electromagnetic waves is one of important issues.

In this paper, we present the propagation characteristics of the high-power microwave guiding in the plasma waveguide. In order to isolate two issues of making the plasma waveguide and investigation of the propagation characteristics of electromagnetic waves in the plasma waveguide, the experiment has used a long and thin glass strip introduced on the axis of the chamber to generate the nonevolving plasma waveguide. Fourier analysis of the axial electric field pattern within the plasma waveguide clearly represents that the dominant wave number of the microwave lies within the range of those estimated for an optical fiber, that is, a dielectric waveguide with a step refractive index profile. The numerical calculations of the radial electric field profile also have been carried out. The results are in fairly good agreement with the results observed in the present experiments.

II. EXPERIMENTAL APPARATUS

The experimental arrangement used in the present studies is shown schematically in Fig. 1. A cylindrical, unmagnetized argon plasma is produced in a stainless-steel chamber of 100 cm length \times 60 cm diameter. The outside surface of the vacuum chamber is covered with a number of multidipole permanent magnets for a plasma confinement. Although there are magnetic field on the inside wall of the vacuum

*Electronic address: hiroakii@cc.utsunomiya-u.ac.jp

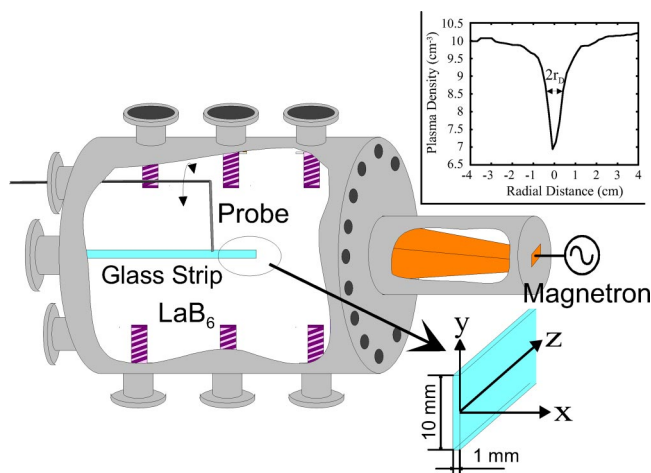


FIG. 1. (Color online) Experimental apparatus used in the present studies.

chamber, a magnetic field free plasma is produced in a stainless-steel chamber by a pulsed discharge between three sets of LaB cathode and the chamber wall (grounded). A typical discharge duration and discharge voltage are 1.5 ms and 180 V, respectively, with the repetition rate of 10 Hz. The base pressure of the chamber is $P_0 \approx 8 \times 10^{-7}$ Torr and an argon gas pressure is adjusted to $P_{Ar} = (3-5) \times 10^{-3}$ Torr by a needle valve. The pulsed microwave has a frequency of $f_0 = \omega_0 / 2\pi = 9$ GHz, maximum power of 250 kW, and a typical pulse duration of $1 \mu\text{s}$ in full width at half maximum (FWHM). The microwave is generated by a magnetron with a repetition rate of 10 Hz and is irradiated into the plasma from the rectangular horn antenna with the aperture area $12 \times 10 \text{ cm}^2$. The antenna is located at the lower end of the plasma density. The plasma density and the rf electric field inside the plasma are measured by a cylindrical probe with a tip of 1 mm length $\times 0.25$ mm diameter, movable along the axis and rotatable in the radial direction. Typical plasma parameters are the maximum electron density $n_{\text{max}} \approx 1.2 \times 10^{12} \text{ cm}^{-3}$ and the electron temperature $T_e \approx 2-3 \text{ eV}$. The ratio of the electric field energy to the plasma energy is estimated to be $\eta \equiv \epsilon_0 E_0^2 / 4n_0 k_B T_e \approx 0.5$, where E_0 is the maximum electric field intensity of the incident microwave measured at the outlet of the horn antenna, n_0 is the electron density there, and k_B is Boltzmann's constant.

The preformed plasma channel is formed by inserting a thin glass strip with 70 cm length $\times 1$ cm width $\times 0.1$ cm thickness at the center of the chamber along the plasma axis. In the present experiments, the glass strip is inserted from the higher density side up to 20 cm from the edge of the horn antenna. Because of the recombination on the glass strip, it acts as a sink and the plasma density is reduced at the surface, growing gradually towards larger radial positions. As the glass strip is present in the chamber for all the time, the stability of the channel production is guaranteed. Thus, the production of the plasma waveguide is highly reproducible in the present study. The width and depth of the desired plasma waveguide can be adjusted by changing the background plasma density. An example of the spatial distribution of preformed plasma channel at $z=20$ cm is shown in the

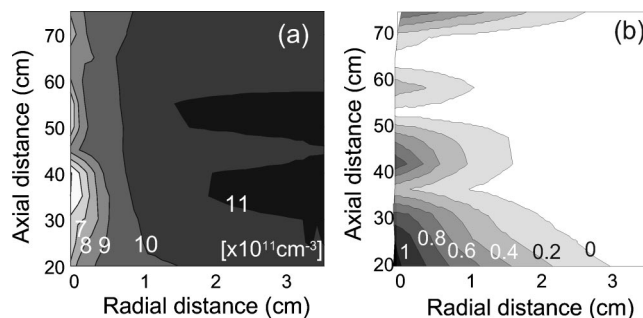


FIG. 2. Contour plot of plasma density and microwave electric field intensity. (a) Contour plot of plasma density in the absence of microwave in r - z plane. (b) Contour plot of microwave electric field intensity within the density channel, where incident power is 250 kW.

inset of Fig. 1 and its full width at half maximum ($2r_D$) perpendicular to the electric field E_y is less than about 10 mm, which is small enough compared with the cut off wavelength ($\lambda_c = \lambda_0 / 2 \approx 16 \text{ mm}$) of the fundamental TE mode in the standard rectangle waveguide. Such measurement is done by rotating the probe from its initial position near the glass strip to away from the strip using slowly moving motor driving system. The electromagnetic wave (EMW) is polarized in the y direction, so that the plasma waveguide is cut off to the EMW in the overdense region because of too narrow waveguide width.

III. EXPERIMENTAL RESULTS

Figure 2(a) shows an example of two-dimensional plasma density distribution in the absence of the incident microwave. As the typical radial profile in the inset of Fig. 1 can be seen symmetric with respect to the chamber axis, all measurements are shown only on one side of the glass strip. In order to control the propagation mode of EMW within the plasma waveguide to be the fundamental TE mode, the dimension of the plasma waveguide perpendicular to the direction of an electric field should be adjusted at least to be half the vacuum wavelength of the incident microwave. It can be clearly seen from Fig. 2(a) that the preformed plasma channel is formed from $z=20$ cm to 75 cm and its width is less than the cutoff wavelength λ_c .

When a microwave pulse is injected into this plasma waveguide, a typical example of two-dimensional distribution of the electric field intensity is shown in Fig. 2(b), where the power of the incident microwave is 250 kW. Although the width of the preformed plasma channel is kept less than the cutoff wavelength, it is observed from Fig. 2(b) that the high-power microwave remains trapped within the plasma waveguide and propagates for about 50 cm into it. Furthermore, the electric field is confined around the axis. The high-power microwave cannot penetrate up to the other end of the chamber from higher radial distances because the plasma density is more than the critical density, as seen in Fig. 2(a). The standing wave formation in the plasma waveguide can be expected to be due to the reflection of microwave energy,

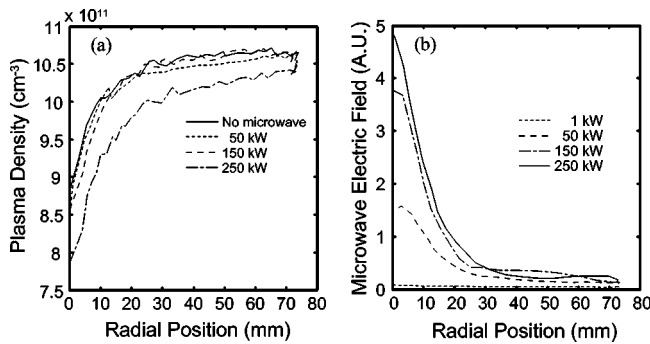


FIG. 3. Radial profiles of (a) plasma density and (b) microwave electric field intensity as a parameter of the incident microwave power at axial position $z=60$ cm.

which has entered the preformed channel, from the end wall of the chamber.

Figure 3 shows the radial profile of the plasma density and of the microwave electric field intensity as a function of the incident microwave power, where the axial position is $z=60$ cm. We can see from Fig. 3(a) that the radial plasma density profile is widened when the microwave is injected into the preformed plasma channel. The radial half width of plasma waveguide Δr_D increases with the incident microwave power. The width at the incident power 250 kW is 8.9 mm, so expansion of the plasma waveguide is almost 90% of the original width, 4.6 mm (in absence of the incident microwave). We can see from Fig. 3(b) that no appreciable penetration is observed when the incident microwave power is below $P=50$ kW, while in case of higher incident power (above 50 kW), the microwave can propagate into the overdense region. In addition, it is clear from Fig. 3(b) that the half width of the electric field distribution becomes narrower with the increase of the incident power, that is, the microwave is confined around the axis of the plasma waveguide. This can be explained by simple laws of optics and the dependence of the refractive index (N) on the plasma density, $N = \sqrt{1 - (\omega_p / \omega_0)^2}$, where $\omega_p = (4\pi n_e |e|^2 / m_e)^{1/2}$ is the plasma frequency with popular notations. As the incident power increases, the plasma waveguide is widened and bored deeper due to the ponderomotive force of the microwave in the plasma waveguide. This makes region of higher refractive index narrower leading to the confinement of the electric field in a smaller radial extent. The result of Fig. 3 shows that the microwave modifies the refractive index of the plasma waveguide. It is evident from Figs. 2 and 3 that the microwave makes a duct by expanding the plasma via the ponderomotive force and propagates into higher density side along the plasma waveguide. Thus, the preformed plasma channel acts as a waveguide to guide the high-power microwave.

Figure 4(a) shows the experimentally observed radial profile of the electric field intensity in the plasma waveguide as a function of the preformed plasma channel width, where the incident microwave power is 250 kW. The data are normalized to the maximum value. For the narrower width, the peak of the electric field distribution is present on the axis of the plasma waveguide. It turns out from Fig. 4(a) that the peak tends to be shifted off axis with the increase of the preformed

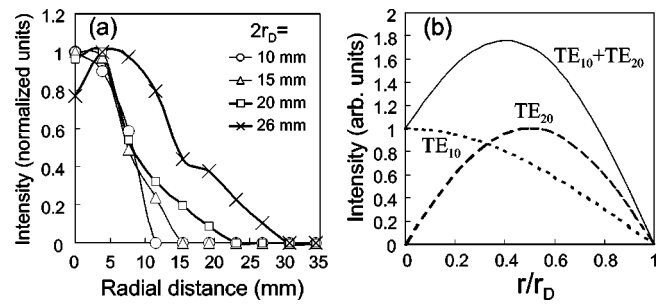


FIG. 4. Radial profiles of electric field as a function of plasma channel width. (a) Normalized radial profile of electric field intensity observed experimentally. Incident microwave power is 250 kW. (b) Radial profile calculated by theory of standard waveguide. Dotted, dashed, and solid lines represent the mode TE₁₀, TE₂₀, and sum of TE₁₀ and TE₂₀, respectively.

channel width. From this result, it is expected that the higher mode of the microwave starts appearing with the increase of the preformed channel width.

In order to investigate the mode structure of propagation in the plasma waveguide in detail, the mode measurements have been carried out for different preformed plasma channel widths. Figure 5(a) shows the wave number spectrum obtained by applying a fast Fourier transformation (FFT) to the data of the axial electric field profile. As seen in Fig. 5(a), a new wave number spectrum $k=0.7$ cm⁻¹ appears within the plasma waveguide for the smallest plasma channel width $2r_D=9$ mm. For comparison, the FFT of the microwave field distribution has been taken when there is no plasma in the chamber and there is a plasma with density less than the critical density 1×10^{12} cm⁻³. An example of the wave number spectrum measured near the glass strip is shown in Fig. 5(b), where the plasma density is, $n \approx 3 \times 10^{11}$ cm⁻³, less than the critical density. The observed dominant wave number spectrum is always close to $k \approx 1.9$ cm⁻¹, which corresponds to the wave number of the incident microwave with the frequency 9 GHz. It is obvious from Fig. 5 that the wave number of the guiding microwave in the plasma waveguide is clearly different from that of the incident microwave. In addition, we can see from Fig. 5(a) that as the width of the preformed density channel is widened the peak shifts to

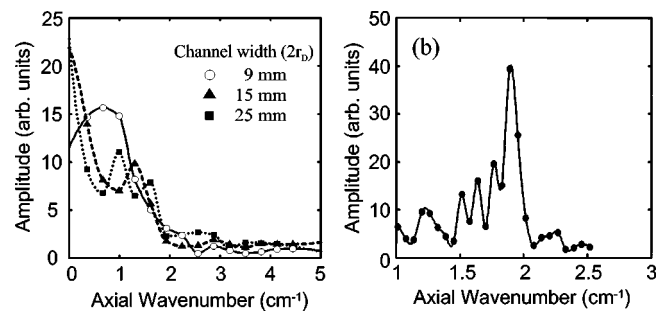


FIG. 5. Wave number spectra obtained by applying a FFT to the data of the electric field intensity for incident power $P=250$ kW. (a) Wave number spectrum of microwave field within the density channels of different widths and (b) wave number spectrum in the presence of plasma less than critical density near the glass strip.

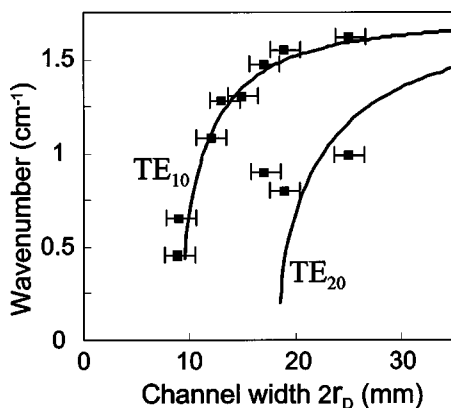


FIG. 6. Dependence of the dominant wave number on the width of plasma channel. The solid squares and the solid line indicate that the experimental wave numbers and the calculated values.

larger wave number and that another peak appears around $k=1 \text{ cm}^{-1}$ for the largest width $2r_D=25 \text{ mm}$.

Figure 6 shows the dependence of the dominant wave number on the width of the preformed plasma channel. The solid squares with error bars indicate the experimentally observed wave numbers. We can see clearly from Fig. 6 that the microwave in the plasma waveguide has two kinds of wave numbers as the plasma channel width becomes more than 15 mm wider. This is in good agreement with the plasma channel width in which the peak of the electric field profile in Fig. 4 is shifted off axis. It is evident from Figs. 4–6 that the microwave propagate through the plasma waveguide at both the fundamental TE mode and the higher order mode when the plasma channel width is $2r_D > 15 \text{ mm}$.

In order to interpret the observed behavior, the identification of propagation modes within the plasma waveguide have to be carried out. Here, one can employ a propagation model approximated in a rectangular dielectric waveguide having step-index profile with refractive indexes N_1 inside and N_2 outside. In addition, we may put $N_2=0$ because the plasma density outside of the channel is overdense. Numerically calculated wave number can be obtained by using the dispersion relationship of the electromagnetic wave in the standard waveguide filled with plasmas: $\omega_0^2 = \omega_p^2 + \omega_c^2 + c^2 k^2$, where ω_c is the cutoff frequency which depends on the cross section size of the waveguide. Using the refractive index $N_1 = \sqrt{1 - \omega_p^2 / \omega_0^2}$, the wave number of the microwave within the plasma waveguide is given by

$$k^2 = k_0^2 N_1^2 - k_c^2,$$

where $k_0 = \omega_0 / c$ and $k_c = \omega_c / c$. The two solid lines in Fig. 6 indicate the calculated wavenumbers (the fundamental mode

TE₁₀ and higher order mode TE₂₀), where the refractive index is assumed to be $N_1=0.9$. It can be seen from Fig. 6 that the experimentally measured wave numbers are in good agreement with the estimated curve. This result represents that when the width of the preformed density channel is narrower than the cutoff wavelength $\lambda_c \approx 16 \text{ mm}$ of the fundamental TE mode, the propagation mode within the plasma waveguide is very close to the fundamental mode TE₁₀ in the standard waveguide and that the higher order mode starts appearing with the increase of the plasma channel width, more than 16 mm.

Next, let us consider a transverse profile of the microwave electric field in the plasma waveguide. Assuming the above mentioned model, the calculation of the transverse profile in the plasma waveguide can be simplified, i.e., equal to that in the standard waveguide. The calculated results are shown in Fig. 4(b). The value of the horizontal axis is normalized at the width of the preformed plasma waveguide. As seen in Fig. 4(b), in case of coexistence with the higher mode TE₂₀ the peak of the electric field is off axis and in comparison with Fig. 4(a), they agree well. Therefore, it is evident from Figs. 4 and 6 that the higher mode observed in present experiments can be regarded as TE₂₀ higher mode.

IV. CONCLUSIONS

We have investigated the mode structure of the guiding microwave in the preformed plasma waveguide. The microwave pulse expands the plasma waveguide by its ponderomotive force and remains trapped within the plasma waveguide and is guided in it. The propagation structure is the fundamental TE mode for the plasma channel width narrower than the cutoff wavelength λ_c of the fundamental TE mode. As the width of the plasma waveguide becomes wider than λ_c , the microwave propagates through the plasma channel at both the fundamental TE mode and the higher mode. The comparisons of the experimentally observed transverse profile of the electric field with the numerical calculations show fairly good agreement for its dependence on the plasma channel width. The results show that it is possible to control the propagation mode in the plasma waveguide by changing the plasma waveguide parameters and to support the more potentiality of the applications with the laser-matter interaction.

ACKNOWLEDGMENTS

This work is supported in part by the Grant-in-Aid for Scientific Research from the Ministry of Education, Science, Sports and Culture, Japan.

- [1] M. Tabak *et al.*, Phys. Plasmas **1**, 1626 (1994).
 [2] D. Korobkin, A. Goltsov, A. Morozov, and S. Suckewer, Phys. Rev. Lett. **81**, 1607 (1998).
 [3] A. Butler *et al.*, Phys. Rev. Lett. **91**, 205001 (2003).

- [4] I. P. Christov, J. Zhou, J. Peatross, A. Rundquist, M. M. Murnane, and H. C. Kapteyn, Phys. Rev. Lett. **77**, 1743 (1996).
 [5] T. Tajima and J. M. Dawson, Phys. Rev. Lett. **43**, 267 (1979).
 [6] E. Esarey, P. Sprangle, J. Krall, and A. Ting, IEEE Trans.

- Plasma Sci. **24**, 252 (1996).
- [7] Y. Nishida, M. Yoshizumi, and R. Sugihara, Phys. Lett. **105A**, 300 (1984); Y. Nishida and T. Shinozaki, Phys. Rev. Lett. **65**, 2386 (1990).
- [8] A. Modena, Z. Najmudin, A. E. Dangor, C. E. Clayton, K. A. Marsh, C. Joshi, V. Malka, C. B. Darrow, C. Danson, D. Neely, and F. N. Walsh, Nature (London) **377**, 606 (1995).
- [9] F. Amiranoff *et al.*, Phys. Rev. Lett. **81**, 995 (1998).
- [10] C. G. Durfee, III, J. Lynch, and H. M. Milchberg, Phys. Rev. E **51**, 2368 (1995).
- [11] V. Malka, E. De Wispelaere, F. Amiranoff, S. Baton, R. Bonadio, C. Coulaud, and R. Haroutunian, Phys. Rev. Lett. **79**, 2979 (1997).
- [12] P. E. Young, M. E. Foord, J. H. Hammer, W. L. Kruer, M. Tabak, and S. C. Wilks, Phys. Rev. Lett. **75**, 1082 (1995).
- [13] C. E. Clayton, K.-C. Tzeng, D. Gordon, P. Muggli, W. B. Mori, C. Joshi, V. Malka, Z. Najmudin, A. Modena, D. Neely, and A. E. Dangor, Phys. Rev. Lett. **81**, 100 (1998).
- [14] Y. Ehrlich, C. Cohen, A. Zigler, J. Krall, P. Sprangle, and E. Esarey, Phys. Rev. Lett. **77**, 4186 (1996).
- [15] F. Dorchies *et al.*, Phys. Rev. Lett. **82**, 4655 (1999).
- [16] T. Hosokai, M. Kando, H. Dewa, H. Kotaki, S. Kondo, N. Hasegawa, N. Nakajima, and K. Horioka, Opt. Lett. **25**, 10 (2000).
- [17] A. Butler, D. J. Spence, and S. M. Hooker, Phys. Rev. Lett. **89**, 185003 (2002).
- [18] I. V. Pogorelsky *et al.*, Appl. Phys. Lett. **83**, 3459 (2003).
- [19] H. Ito, Y. Nishida, and N. Yugami, Phys. Rev. Lett. **76**, 4540 (1996); H. Ito, N. Yugami, and Y. Nishida, J. Plasma Fusion Res. **74**, 369 (1998).